The neutron halo structure of ^{17}B studied with the relativistic Hartree-Bogoliubov theory*

JI Juan-Xia(姬娟霞)[1,2;1)] LI Jia-Xing(李加兴)[1,2;2)] HAN Rui(韩瑞)[1]
WANG Jian-Song(王建松)[2] HU Qiang(胡强)[2]

[1] School of Physical Science and Technology, Southwest University, Chongqing 400715, China
[2] Institute of Modern Physics, Chinese Academy of Sciences, Lanzhou 730000, China

Abstract: The properties of neutron-rich boron isotopes are studied in the relativistic continuum Hartree-Bogoliubov theory in coordinate space with NL-SH, PK1 and TM2 effective interactions. Pairing corrections are taken into account by a density dependent force of zero range. The binding energies calculated for these nuclei agree with the experimental data quite well. The neutron-rich nucleus ^{17}B has been predicted to have a two-neutron halo structure in its ground state. The halo structure of ^{17}B is reproduced in a self-consistent way, and this halo is shown to be formed by the valence neutron level $2s_{1/2}$.

Key words: neutron-rich boron isotopes, halo structure, RCHB theory, neutron halo

PACS: 21.10.Dr, 21.10.Gv, 21.60.Jz **DOI:** 10.1088/1674-1137/36/1/007

1 Introduction

Since the advent of radioactive nuclear beam facilities, the exotic nuclei far from the β-stability line have been studied extensively and many new phenomena, such as neutron skin, neutron- and proton-halo, and a change of magic numbers, have been observed [1–6]. After the neutron halo in ^{11}Li was discovered [1, 7], the existence of the neutron halo in some neutron-rich light nuclei was suggested. The halo nucleus exhibits an extended density distribution, a sudden rise in the interaction cross sections, a narrow fragment momentum distribution, and so on. The investigation of the halo structure has therefore become a hot topic in the field of radioactive nuclear beam physics.

The electric and magnetic moments of neutron-rich boron isotopes show an interesting dependence on the neutron number [8]. The neutron dependence of the electromagnetic properties is caused by some structural changes, such as the development of cluster and halo structures. The properties of neutron-rich boron isotopes have been studied with the antisymmetrized molecular dynamics (AMD) model [9, 10]. The ^{17}B was predicted to have a halo structure with the core ^{15}B, plus two valence neutrons [11–19]. It is first pointed out that the long-range effective potential indicates the effect of the three-body correlation and leads to neutron halos in ^{17}B [12]. On the experimental side, several results have confirmed the halo structure of ^{17}B [16–18]. The two-neutron separation energy S_{2n} is known to be 1.39 ± 0.14 MeV for ^{17}B. The interaction cross section for ^{17}B on a carbon target at 880 A MeV was measured to be 1118 ± 22 mb at FRS [15]. The effective root-mean-square (rms) matter radii of ^{17}B were about 2.90 and 2.99 fm from σ_I by two different methods: a Glauber-type calculation based on the optical limit approximation and a few-body reaction model. A Glauber-type analysis of the data provides clear evidence of a two-neutron halo structure in ^{17}B [16]. In the experiment performed at RIKEN, the density distribution of ^{17}B shows a large

Received 18 March 2011

∗ Supported by National Natural Science Foundation of China (11075133, 10205019, 11075190), Fundamental Research Funds for the Central Universities (XDJK2010D005, XDJK2010C049), Knowledge Innovation Program of Chinese Academy of Sciences (KJCX2-YW-N44) and Open Research Program at Large Scale Facility of Chinese Academy of Sciences (O903010YKF)

1) E-mail: j812@swu.edu.cn

2) E-mail: lijx@swu.edu.cn

tail, which indicates the existence of a two-neutron halo structure [17].

Relativistic mean field theory has achieved great success in describing finite nuclei and nuclear matter. The relativistic continuum Hartree-Bogoliubov (RCHB) theory [21, 22], which extends the RMF theory via the supplementation of the Bogoliubov transformation to treat the pairing correlations and solves the RHB equations in coordinate space, has had great success in the analysis of halo and giant halo structures in atomic nuclei [23, 24]. In comparison with traditional BCS theory, RCHB theory can properly take into account the coupling to continuum, which is crucial for the description of dripline nuclei. As shown in Ref. [20], the scattering of Cooper pairs into the continuum containing low-lying resonances of small orbital angular momentum plays an important role in the formation of neutron halos, e.g. in ^{11}Li.

In the present work, we study the properties of ^{17}B, as well as other boron isotopes, with the RCHB theory. The main goal of this work is to understand the formation of the halo structure of ^{17}B.

2 Formalism

In RCHB theory, the particle-hole (ph) and particle-particle (pp) correlations are described in a unified way on a mean field level by using two average potentials: the self-consistent mean field that encloses all the long-range ph correlations, and a pairing field Δ which sums up the pp correlations. The ground state of the nucleus is described by a generalized Slater determinant $|\Phi\rangle$ that represents the vacuum with respect to the independent quasiparticles (α^+_κ), which are related to the single-nucleon (c^+_l) and annihilation c_l operators through the unitary Bogoliubov transformation

$$\alpha^+_\kappa = \sum_\mathrm{l} U_{\mathrm{l}\kappa} c^+_\kappa + V_{\mathrm{l}\kappa} c_\mathrm{l}, \tag{1}$$

where U and V are the Hartree-Bogoliubov wave functions determined by the solution of the RCHB equation. In coordinate representation, this is

$$\begin{pmatrix} h_\mathrm{D} - m - \lambda & \Delta \\ -\Delta^* & -h^*_\mathrm{D} + m + \lambda \end{pmatrix} \times \begin{pmatrix} U_\kappa(\boldsymbol{r}) \\ V_\kappa(\boldsymbol{r}) \end{pmatrix} = E_\kappa \begin{pmatrix} U_\kappa(\boldsymbol{r}) \\ V_\kappa(\boldsymbol{r}) \end{pmatrix}, \tag{2}$$

where m is the nucleon mass, and the chemical potential λ is determined by the particle number subsidiary condition, in order that the expectation value of the particle number operator in the ground state equals the number of nucleons. The column vectors denote the quasiparticle wave functions, and E_κ are the quasiparticle energies. The Dirac Hamiltonian $\hat{h}_\mathrm{D}$, in the usual meson-exchange representation and for the stationary case with time-reversal symmetry,

$$\hat{h}_\mathrm{D} = \boldsymbol{\alpha}\cdot\boldsymbol{p} + \beta(m + g_\sigma\sigma) + g_\omega\omega^0 + e\frac{1-\tau_3}{2}A^0 \tag{3}$$

contains the mean-field potentials of the isoscalar scalar σ-meson, the isoscalar vector ω-meson, and the isovector vector ρ meson, as well as the electrostatic field A^0. The RHB equations have to be solved self-consistently, with the potentials determined in the mean field approximation from the solutions of Klein-Gordon equations.

The pairing correlations are taken into account by a density-dependent δ force of the form [4]

$$V^{\mathrm{pp}}(r_1, r_2) = V_0\delta(r_1, r_2)\frac{1}{4}(1-\sigma_1\cdot\sigma_2)\left[1 - \frac{\rho(r)}{\rho_0}\right], \tag{4}$$

where ρ_0 is taken as 0.152 fm^{-3} as usual.

The pairing field $\hat{\Delta}$ in Eq. (2) is defined

$$\Delta_{ab}(\boldsymbol{r}, \boldsymbol{r}') = \frac{1}{2}\sum_{c,d} V_{abcd}(\boldsymbol{r}, \boldsymbol{r}')\kappa_{cd}(\boldsymbol{r}, \boldsymbol{r}'), \tag{5}$$

where a, b, c, d denote the quantum numbers that specify the single-nucleon states. $V_{abcd}(\boldsymbol{r}, \boldsymbol{r}')$ are the matrix elements of a general two-body pairing interaction, and the pairing is defined

$$\kappa_{cd}(\boldsymbol{r}, \boldsymbol{r}') = \sum_{E_\kappa > 0} U^*_{c\kappa}(\boldsymbol{r}) V_{d\kappa}(\boldsymbol{r}'). \tag{6}$$

In order to describe the coupling between the bound and continuum states more exactly, the RHB equations and the equations for the meson fields should be solved in coordinate space, and one arrives at the RCHB theory. For details of the RCHB formalism and its applications, see Refs. [21, 22].

3 Numerical details and results

The RCHB equations are solved in a self-consistent way by the shooting method and the Runge-Kutta algorithm with a step size of 0.1 fm using proper boundary conditions in a spherical box of radius $R = 20$ fm. The number of continuum levels is restricted by introducing a cutoff energy of 120 MeV. More details can be found in Ref. [22].

Three nonlinear effective interactions, NL-SH [25], PK1 [26] and TM2 [27] are adopted. Pairing is neglected for the five protons, and the pairing strength V_0 for the neutrons is determined by fitting to the experimental binding energies of ^{17}B.

In Fig. 1 we plot the total binding energy of ^{17}B as a function of the neutron pairing strength from the RCHB calculations with the effective interactions of NL-SH, PK1 and TM2. As expected, the total binding energy increases with the pairing strength $V_{\rm n}$. Compared with the experimental binding energies of ^{17}B, the pairing strengths $V_{\rm n}$ = 326, 307 and 302 MeV·fm^{-3} are adopted in the following calculations for NL-SH, PK1 and TM2, respectively.

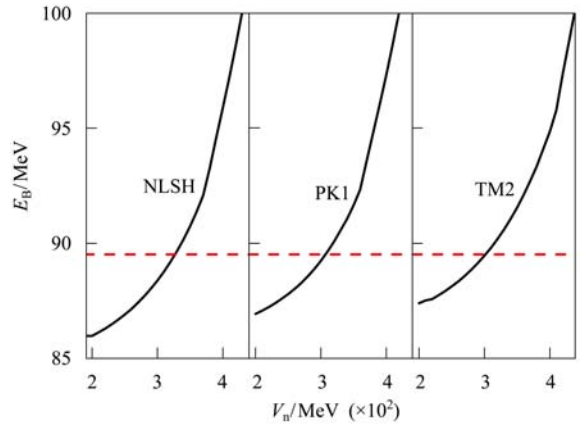

Fig. 1. (color online) The total binding energy ($E_{\rm B}$) as a function of neutron pairing strength in the RCHB calculations, with the effective interactions of NL-SH (left), PK1 (middle) and TM2 (right) for ^{17}B. The experimental data of binding energy $E_{\rm exp}$ are indicated as horizontal lines, correspondingly.

In Fig. 2 we show the calculated binding energies $E_{\rm B}$ and the rms matter radii for the B isotopes with the mass numbers $A = 10$ to $A = 19$, and compare them with the experimental values [28] and the results calculated with the AMD method [29]. The binding energies of boron isotopes are reproduced within the RCHB framework quite well, as are the experimental data of the rms matter radii of B isotopes. This shows that all three effective interactions predicted very similar properties of B isotopes. However, compared with PK1 and TM2, the NL-SH parameter gives better agreement. The rms matter radii of B isotopes are practically constant for $N < 8$, however there is a large increase in the radius from ^{15}B to ^{17}B. A similar rate of increase is seen from ^{17}B to ^{19}B.

The proton and neutron densities in ^{13}B and ^{17}B from the RCHB calculations with the NL-SH, PK1 and TM2 effective interactions are shown in Fig. 3. From this figure it can be clearly seen that the neutron density of ^{17}B has a long tail respect to the proton density compared with the neutron magic nucleus ^{13}B. This means that ^{17}B is a neutron-halo nucleus.

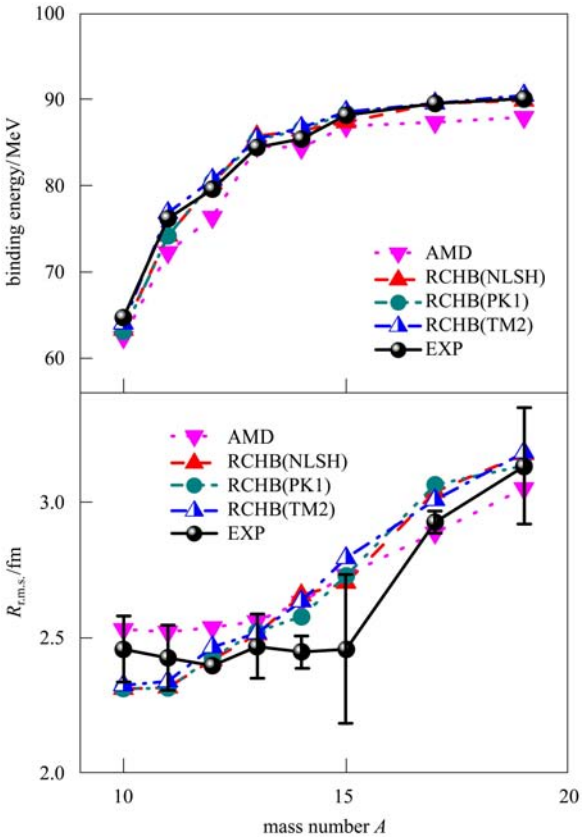

Fig. 2. (color online) The binding energies (upper part) and matter radii (lower part) for B isotopes calculated with the RCHB are compared with experimental values and the results calculated with AMD.

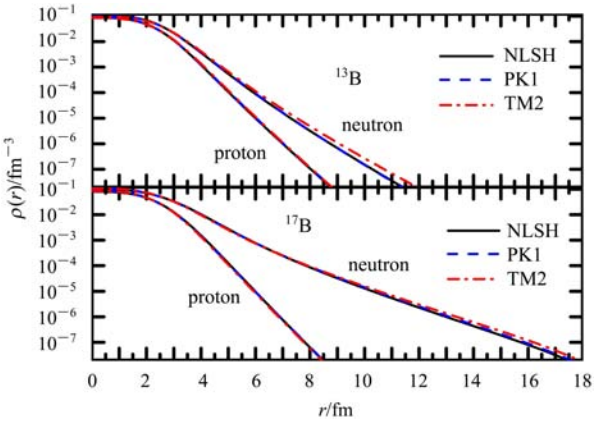

Fig. 3. (color online) The density distributions of protons and neutrons in ^{13}B and ^{17}B from the RCHB calculations with the NL-SH (black solid line), PK1 (blue dashed line) and TM2 (red dash-dotted line) effective interactions, respectively.

In Fig. 4 we show the mean field potentials of the neutron and proton for ^{13}B and ^{17}B, together with the energy levels $\epsilon_{\rm n} = \langle n \mid h \mid n \rangle$ in the canonical basis. ^{13}B is a neutron magic nucleus with $N = 8$, and

the Fermi level ($\lambda_n = -4.27$ MeV) is away from the continuous spectrum. The $1s_{1/2}$, $1p_{3/2}$ and $1p_{1/2}$ levels are filled by eight neutrons. For the usual stable nuclei, the $1d_{5/2}$ level is lower than the $2s_{1/2}$ level.

For ^{17}B, we clearly see that the neutron Fermi surface ($\lambda_n = -0.91$ MeV) is very close to the continuum limit in close vicinity to the $\nu 2s_{1/2}$ and $\nu 1d_{5/2}$ levels, in addition to the fact that the $\nu 2s_{1/2}$ level is lower than the $\nu 1d_{5/2}$ level, and the pairing corrections cause a partial occupation of both the $\nu 2s_{1/2}$ and $\nu 1d_{5/2}$ levels.

In Table 1 we present the neutron single particle energy and occupation probability in canonic basis, and the corresponding rms radius from the RCHB calculations with NL-SH, PK1 and TM2 effective interactions. Due to the large orbital angular momentum and correspondingly large centrifugal barrier, the neutron halo of ^{17}B cannot be formed by level $1d_{5/2}$. The rms radius of level $2s_{1/2}$ is large. The neutron halo is formed mostly by the occupied valence neutron level $2s_{1/2}$, with small orbital angular momentum and a correspondingly small centrifugal barrier.

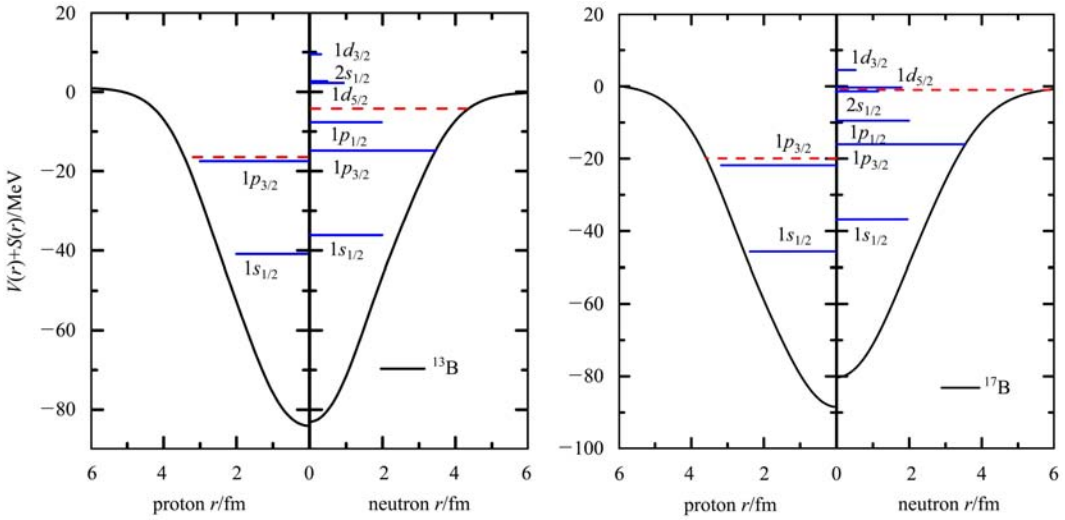

Fig. 4. (color online) The single particle levels of ^{13}B (left panel) and ^{17}B (right panel) calculated by RCHB with the NL-SH effective interaction. The mean field potentials $S+V$ for the proton (left sub-panel) and neutron (right sub-panel) are shown by the solid curves. The chemical potential is given by a dashed line. The energy levels in the canonical basis are indicated by horizontal lines with various lengths proportional to the occupation of the corresponding orbit (except for the levels $\nu 1d5/2$, $\nu 2s1/2$ and $\nu 1d3/2$ of ^{13}B, whose lengths are proportional to the occupation of the corresponding orbit times 10^8).

Table 1. The neutron single particle energy (ε_κ), occupation probability (v_κ^2) and corresponding rms radius ($\sqrt{\langle r^2\rangle_\kappa}$) from the RCHB calculations with NL-SH, PK1 and TM2 effective interactions for the ground-state of ^{17}B.

ψ_{nlj}	NLSH			PK1			TM2		
	ε_κ	v_κ^2	$\sqrt{\langle r^2\rangle_\kappa}$	ε_κ	v_κ^2	$\sqrt{\langle r^2\rangle_\kappa}$	ε_κ	v_κ^2	$\sqrt{\langle r^2\rangle_\kappa}$
$1s_{1/2}$	−36.680	0.999	1.970	−35.950	0.999	1.963	−37.340	0.999	1.987
$1p_{3/2}$	−15.920	0.993	2.756	−15.380	0.993	2.784	−15.880	0.994	2.804
$1p_{1/2}$	−9.431	0.979	3.078	−9.363	0.980	3.103	−8.457	0.979	3.211
$2s_{1/2}$	−1.391	0.654	4.952	−1.665	0.730	4.934	−1.348	0.673	5.084
$1d_{5/2}$	−0.445	0.402	3.869	−0.359	0.376	3.801	−0.563	0.407	3.853

4 Summary

In summary, the ground state properties of ^{17}B have been studied in the context of RCHB theory with the NL-SH, PK1 and TM2 effective interactions. A density-dependent δ-force has been used for the pairing channel. The pairing strength for the neutron is determined by fitting to the experimental binding energies.

A neutron halo structure was found in the ground state of ^{17}B from the RCHB calculations with the three effective interactions. The neutron halo is formed mostly by the occupied valence proton level $2s_{1/2}$ with a small centrifugal barrier. The effects of pairing correlations make the neutron distribution more extended, by scattering protons partially to $1d_{5/2}$ orbits.

We thank Prof. Jie Meng for providing the RCHB code and acknowledge Jiangming Yao for helpful discussions.

References

1 Tanihata I et al. Phys. Rev. Lett., 1985, **55**: 2676
2 Riisager K. Rev. Mod. Phys., 1994, **66**: 1105
3 Hansen P G, Jensen A S, Jonson B. Ann. Rev. Nucl. Sci., 1995, **45**: 591
4 Tanihata I. Prog. Part. Nucl. Phys., 1995, **35**: 505
5 Tanihata I. J. Phys. G: Nucl. Part. Phys., 1996, **76**: 215
6 Jensen A S et al. Rev. Mod. Phys., 2004, **76**: 215
7 Hansen P G, Jonson B. Eur. Phys. Lett., 1987, **4**: 409
8 Okuno H et al. Hyperfine Interact, 1993, **78**: 97
9 Horiuchi H, Kanada-En'yo Y. Nucl. Phys. A, 1997, **616**: 394c–405c
10 Takemato H et al. Prog. Theor. Phys., 1999, **101**: 101
11 REN Z Z, Xu G G. Phys. Lett. B, 1990, **252**: 3
12 REN Z Z. J. Phys. G, 1994, **20**: 1185
13 REN Z Z, Carstoiu F. HEP & NP, 1995, **19**: 6 (in Chinese)
14 Kanada-En'yo Y, Horiuchi H. Phys. Rev. C, 1995, **252**: 647–662
15 Suzuki T et al. Nucl. Phys. A, 1999, **658**: 313–326
16 Suzuki T et al. Phys. Rev. Lett., 2002, **89**: 012501
17 Yamaguchi Y et al. Phys. Rev. C, 2004, **70**: 054320
18 HU Z G et al. Sci. China Ser. G-Phys. Mech. Astron., 2008, **517**: 781–787
19 WANG M et al. Chin. Phys. C (HEP & NP), 2008, **32**: 548–551
20 MENG J, RING P. Phys. Rev. Lett., 1996, **77**: 3963
21 MENG J et al. Prog. Part. Nucl. Phys., 2006, **57**: 470
22 MENG J. Nucl. Phys. A, 1998, **635**: 3
23 MENG J, RING P. Phys. Rev. Lett., 1998, **80**: 460
24 ZHANG S Q et al. Chin. Phys. Lett., 2002, **19**: 312
25 Sharma M M et al. Phys. Lett. B, 1993, **312**: 377
26 LONG W H et al. Phys. Rev. C, 2004, **69**: 034319
27 Sugahara Y, Toki H. Nucl. Phys. A, 1994, **579**: 557
28 Audi G, Wapstra A H, Thibault C. Nucl. Phys. A, 2003, **729**: 337–676
29 Takemoto H, Horiuchi H, Ono A. Phys. Rev. C, 2001, **63**: 034615